Mon. Not. R. Astron. Soc. **397,** 1073–1083 (2009) doi:10.1111/j.1365-2966.2009.15069.x

NGC 2587: a sparse open cluster projected on to a populous star field

Andrés E. Piatti,[1⋆] Juan J. Clariá[2⋆] and Andrea V. Ahumada[2,3⋆]

[1]*Instituto de Astronomía y Física del Espacio, CC 67, Suc. 28, 1428 Ciudad de Buenos Aires, Argentina*
[2]*Observatorio Astronómico, Universidad Nacional de Córdoba, Laprida 854, X5000BGR Córdoba, Argentina*
[3]*European Southern Observatory, Alonso de Córdova 3107, Santiago, Chile*

Accepted 2009 May 7. Received 2009 May 6; in original form 2009 March 20

ABSTRACT

We present CCD photometry in the Johnson U, B and V and Kron–Cousins I passbands for the open cluster NGC 2587. The sample consists of 4406 stars reaching down to $V \sim 21.0$. We developed a new method to clean statistically the colour–magnitude diagrams. NGC 2587 appears to be a sparse, relatively bright open cluster, with a few tens of members projected on to a populous star field. The comparatively bright F7/8 II type star HD 70927, located close to the cluster centre, seems not to be a member. Our analysis suggests that NGC 2587 is slightly younger than the Hyades and probably of solar metallicity. A cluster radius of roughly 8 arcmin was estimated from the radial stellar density profile. From 18 probable cluster members with measured proper motions, we derive the following mean values for NGC 2587: $\mu_\alpha = -4.3 \pm 3.6\,\mathrm{mas\,yr^{-1}}$ and $\mu_\delta = -2.5 \pm 3.4\,\mathrm{mas\,yr^{-1}}$. Adopting the theoretical metal content $Z = 0.02$, which provides the best global fit, we derive a cluster age of 500^{+60}_{-50}. Simultaneously, colour excesses $E(B-V) = 0.10$ and $E(V-I) = 0.15$ and an apparent distance modulus of $V - M_V = 12.50$ are obtained. The interstellar extinction in the cluster direction is found to follow the normal law. NGC 2587 is located at a distance of (2.70 ± 0.70) kpc from the Sun and ∼9.8 kpc from the Galactic centre.

Key words: techniques: photometric – galaxy: open clusters and associations: general – Galaxy: open clusters and associations: individual: (NGC 2587).

1 INTRODUCTION

Intermediate-age and old Galactic open clusters (OCs) range widely in terms of Galactocentric distances, ages and metallicities (Friel 1995). They are located in the disc of the Galaxy and are extremely useful as probes of both age and metallicity in the dynamical and chemical evolution of the Galactic disc. Research dealing with possible abundance gradients in the disc and the age–metallicity relationship for the Galaxy (e.g. Chen, Hou & Wang 2003; Bonatto et al. 2006) requires high quality data on the greatest possible number of OCs ranging vastly in age.

This paper is part of a series devoted to the study of some unstudied or poorly studied OCs, located in different Galactic radii. We are particularly interested in studying intermediate-age and/or old OCs. Our aim is to obtain good-quality CCD photometric data not only to produce a larger sample of studied OCs but also to derive their fundamental properties accurately, using the most recently computed theoretical isochrones. We have already reported results on several relatively young (e.g. Piatti, Clariá & Ahumada 2006), intermediate-age (e.g. Piatti, Clariá & Ahumada 2004a) and old (e.g. Piatti, Clariá & Ahumada 2004b) OCs.

The cluster of our current interest is NGC 2587, also designated as C0821-293, Cr 184 (Collinder 1931) or BH 30 (van den Bergh & Hagen 1975). It is number 706 in the catalogue of Alter, Ruprecht & Vanisek (1970). NGC 2587 is located in a rich star field in Puppis at equatorial coordinates $\alpha_{2000} = 8^{\mathrm{h}}23^{\mathrm{m}}.4$, $\delta_{2000} = -29^\circ 30'.5$ and Galactic coordinates $l = 249^\circ.46$ and $b = +04^\circ.47$. According to these coordinates, this object is the same as the one named ESO 431-SC007 (Lauberts 1982). The Lund Catalogue of Open Cluster Data (Lyngå 1987) describes NGC 2587 as a slightly concentrated, moderately rich cluster, with about 40 members and an angular diameter of 10 arcmin as measured from the POSS chart. More recently, Archinal & Hynes (2003) refer to this cluster as belonging to Trumpler class III-2m (Trumpler 1930), i.e. a detached cluster with no central concentration and a medium range in the brightness distribution of the stars. NGC 2587 presents the comparatively bright star HD 70927 ($V = 9.03$) close to its centre.

As far as we are aware, no photometric study has yet been published about this relatively bright cluster. This is one of the reasons that justify the current study. Although Bustos Fierro (Bustos Fierro

⋆E-mail: andres@iafe.uba.ar (AEP); claria@oac.uncor.edu (JJC); aahumada@eso.org (AVA)

2007, hereafter BF07) measured proper motions within a $2^\circ \times 2^\circ$ field of a *Carte du Ciel* plate containing NGC 2587, he neither determined the cluster parameters nor verified its physical reality. On the other hand, an integrated spectrum, recently obtained by Palma et al. (2008) by scanning the slit across NGC 2587 in the north-south direction, led them to conclude that this is an unreddened intermediate-age cluster of ∼1 Gyr. Since the stellar field over which NGC 2587 is projected is certainly very rich, it is quite probable that the cluster integrated light is strongly contaminated by the presence of foreground/background stars. It is also probable that the comparatively bright F7/8 II type star (Houk & Cowley 1975) HD 70927 could be contaminating the integrated spectrum. In either case, the parameters derived by Palma et al. (2008) could be not reflecting the cluster properties.

The present work attempts at shedding light on the nature of this object by using high-quality photometric data and the proper motions available for the cluster region. In this study, we develop a new method to discriminate carefully cluster members from non-members and determine the cluster reddening, distance, age and metallicity.

In Section 2, we describe the observational material and the data reduction. The quality of the data is analysed in Section 3. A detailed analysis of the photometric data is presented in Section 4. In particular, we describe the colour–magnitude diagrams (CMDs) and propose a new method to clean them. In Section 5, we determine the fundamental cluster parameters through the fitting of theoretical isochrones, while in Section 6 we present an analysis of the available proper motions in the cluster field. A short summary of our main conclusions is given in Section 7.

2 OBSERVATIONS AND DATA REDUCTIONS

We obtained CCD images of the cluster field with the $UBVI_{KC}$ filters and the 0.9-m telescope at Cerro Tololo Inter-American Observatory (CTIO, Chile) during the night of 2000 December 28–29. The telescope – equipped with the 2048 × 2048 pixel Tektronix 2K No. 3 CCD, with a pixel size of 24 μm – yielded a scale on the chip of 0.4 arcsec pixel^{-1} (focal ratio f/13.5) and a visual field of 13.6 × 13.6 arcmin^2. We controlled the CCD through the CTIO ARCON 3.3 data acquisition system in the standard quad amplifier mode. The logbook of observations is provided in Table 1. At the beginning of the observing night, we obtained a series of bias and dome and sky flat-field exposures per filter to calibrate the CCD instrumental signature. In order to standardize our photometry, we carried out observations of standard stars of the selected areas PG0231+051, 92 and 98 of Landolt (1992). The selected standard stars cover a wide colour range. In particular, stars in the selected area PG0231+051 were observed at low and high air masses to adjust the extinction coefficients properly. By the end of the night, we had collected 37 different measures of magnitude per filter for the selected standard star sample.

Table 1. Observations log of NGC 2587.

Filter	Exposure (s)	Airmass	Seeing (arcsec)
U	10	1.04	1.4
U	60	1.06	1.3
U	450	1.07	1.5
B	20	1.01	1.5
B	60	1.01	1.3
B	360	1.01	1.4
V	10	1.02	1.5
V	20	1.03	1.3
V	200	1.03	1.6
I	10	1.03	1.4
I	10	1.04	1.3
I	90	1.04	1.4

We reduced the U, B, V, I_{KC} images at the Instituto de Astronomía y Física del Espacio (Argentina) with IRAF[1] using the QUADPROC package. The procedure included the bias subtraction of all the images and the flat fielding of both standard and programme field images. Next, weighted combined signal-calibrator frames were employed. The resulting processed images turned out to be satisfactorily flat. We then derived the instrumental magnitudes for the standard stars from aperture photometry using DAOPHOT/IRAF routines (Stetson, Davis & Crabtree 1990). We obtained the following transformation equations between instrumental and standard magnitudes through least square fits:

$$u = (4.371 \pm 0.118) + U + (0.573 \pm 0.097)X_U - (0.055 \pm 0.015)(U - B), \quad (1)$$

$$b = (2.839 \pm 0.057) + B + (0.262 \pm 0.047)X_B + (0.107 \pm 0.009)(B - V), \quad (2)$$

$$v = (2.757 \pm 0.054) + V + (0.081 \pm 0.043)X_V - (0.015 \pm 0.009)(B - V), \quad (3)$$

$$v = (2.754 \pm 0.056) + V + (0.082 \pm 0.045)X_V - (0.011 \pm 0.008)(V - I), \quad (4)$$

$$i = (3.744 \pm 0.055) + I + (0.018 \pm 0.043)X_I - (0.013 \pm 0.010)(V - I), \quad (5)$$

where X represents the effective air mass, and capital and lowercase letters stand for standard and instrumental magnitudes, respectively. The coefficients were derived through the IRAF routine FITPARAM, resulting in rms errors of 0.039 for u, 0.024 for b, 0.026 for v and 0.031 for i. Note that we performed two independent v transformations – one with $B - V$ and another with $V - I$ – in order to take into account stars observed only in the B or I images. Fig. 1 shows the differences between the calibrated and standard values obtained for the observed standard stars, while Table 2 provides the calibrated magnitude and colours for these stars, along with their photometric errors and residuals. Only a fragment of this table is presented here as a guidance, regarding its form and content. The full table is available in the online version of the article (see Supporting Information).

The instrumental magnitudes for stars in the NGC 2587 field were obtained from point-spread function (PSF) fits using stand-alone versions of the DAOPHOT[2] and ALLSTAR[2] programmes, which provided us with x and y coordinates and instrumental u, b, v and i magnitudes for all stars identified in each field. For each frame, a quadratically varying PSF was derived from a selected star sample, which contained the brightest, least contaminated stars. We then

[1] IRAF is distributed by the National Optical Astronomy Observatories, which is operated by the Association of Universities for Research in Astronomy, Inc., under contract with the National Science Foundation.
[2] Programme kindly provided by P. B. Stetson.

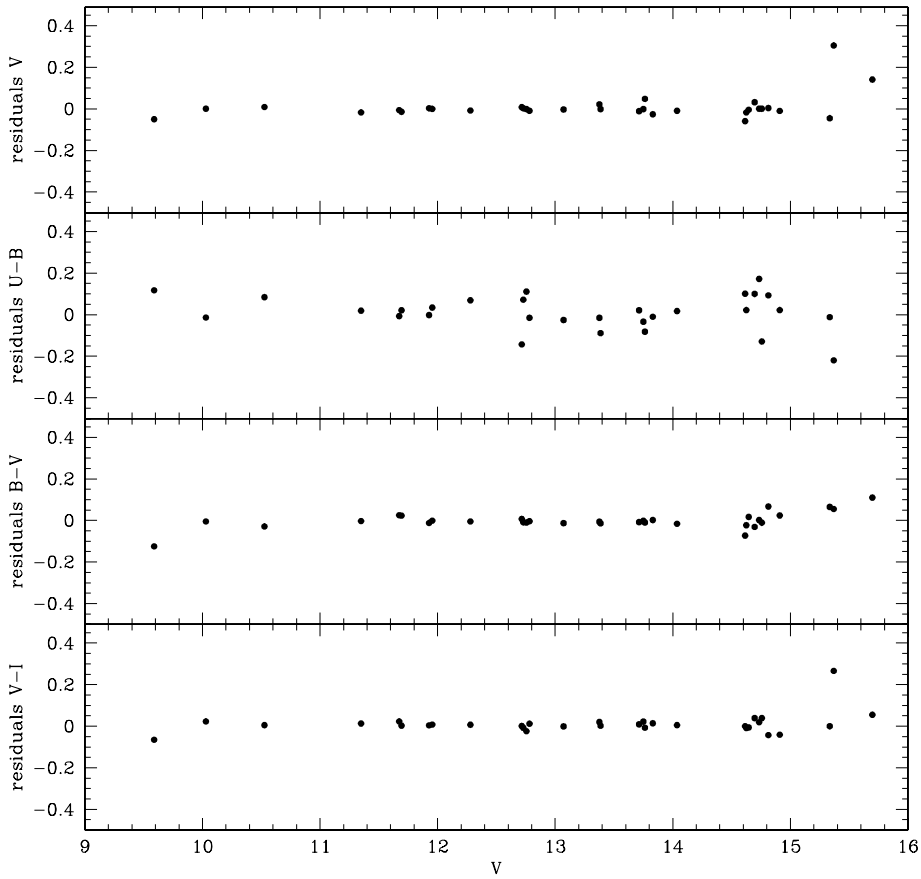

Figure 1. Residuals (calibrated standard values) for the observed standard stars.

used ALLSTAR programme to apply the resulting PSF to the identified stellar objects and to create a subtracted image, which was used to find and measure magnitudes of additional fainter stars. The PSF magnitudes were determined using the aperture magnitudes yielded by PHOT as zero points. This procedure was repeated three times for each frame. Next, we computed aperture corrections from the comparison of PSF and aperture magnitudes using the subtracted neighbour PSF star sample.

Next, we separately combined all the measures for the shorter and longer *ubvi* exposure sets using the stand-alone DAOMATCH[2] and DAOMASTER[2] programmes. We thus obtained three tables which list, in succession, the running number of stars, the x and y coordinates, the u, b, v and i magnitudes and the respective observational errors for each measured star. Note that stars without v magnitudes were excluded from the tables. The standard magnitudes and colours for all the measured stars were computed through equations (1) to (5). Once we obtained the standard magnitudes and colours, we built a master table containing the average of V, $U-B$, $B-V$ and $V-I$, their errors $\sigma(V)$, $\sigma(U-B)$, $\sigma(B-V)$ and $\sigma(V-I)$ and the number of observations for each star, respectively. Whenever there was only one measure of the magnitude and colours, we adopted the corresponding observational error. Table 3 provides the magnitudes and colours for a total of 4406 stars measured in the field of NGC 2587. Only a fragment of this table is presented here as a guidance, regarding its form and content. The complete table, however, is available on the online version of the article (see Supporting Information). Fig. 2 shows the 200-s exposure V image obtained for the stars in the field of NGC 2587.

3 DATA QUALITY AND SCOPES

A simple inspection of Table 3 shows that only 7 per cent of the measured stars have $U-B$ colours, as it usually happens whenever an observed field is quite reddened or when its stars are intermediate-age or old. The 14 and 16 per cent of the total number of stars with $B-V$ and $V-I$ colours, respectively, have three measures. They extend from the brightest limit down to $V = 18.5$ and 19.0 mag, respectively. The 22 and 21 per cent of the stars with $B-V$ and $V-I$ colours have two measures and cover V ranges from 14.0 to 19.0 mag and from 14.0 to 19.5 mag, respectively. The 64 and 63 per cent of the stars have only one measure in $B-V$ and $V-I$. All these stars are fainter than $V = 15.0$ mag and they reach the photometric magnitude limits at $V \sim 21$ mag. According to this crude statistics, the stars lying within the ∼4 brightest out of the ∼10 mag range along which our photometry extends, were measured two and three times. At the same time, we have approximately more than 60 percent of the measured stars with one measure distributed within the six faintest magnitudes reached. Such a result reveals that the field of NGC 2587 has plenty of stars that probably constitute the cluster background.

The behaviour of the photometric errors provided by the standard deviation of the mean for the V magnitude and $U-B$, $B-V$ and $V-I$ colours as a function of V is shown in Table 4. To derive such trends, we have considered all stars regardless of the number of observations. By using photometric errors provided by DAOPHOT (only one measure per star), we obtained similar behaviours with a reasonably smaller intrinsic scatter. Conversely, since the stars with

Table 2. Calibrated *UBVI* data of standard stars. This is a sample of the full table, which is available in the online version of the article (see Supporting Information).

ID	V (mag)	$\sigma(V)$ (mag)	Res(V) (mag)	$U-B$ (mag)	$\sigma(U-B)$ (mag)	Res$(U-B)$ (mag)	$B-V$ (mag)	$\sigma(B-V)$ (mag)	Res$(B-V)$ (mag)	$V-I$ (mag)	$\sigma(V-I)$ (mag)	Res$(V-I)$ (mag)
...	...	...	...	...	...	...	...	...	...	...	...	.
PG0231+051-D	14.036	0.006	−0.009	1.104	0.011	−0.016	1.029	0.021	0.017	1.251	0.007	0.005
SA92-433	11.673	0.001	−0.006	0.630	0.001	0.025	0.117	0.002	−0.007	0.693	0.001	0.023
SA98-671	13.386	0.004	−0.001	0.982	0.005	−0.014	0.808	0.009	−0.089	1.069	0.006	0.002
...	...	...	...	...	...	...	...	...	...	...	...	.
...	...	...	...	...	...	...	...	...	...	...	...	.

two and three measures cover the brightest dynamic magnitude range, they are the most appropriate ones to derive astrophysical information. In addition, the knowledge of the behaviour of the photometric errors with the magnitude for these stars, allows us to rely on the accuracy of the morphology and position of the main cluster features in the CMDs.

4 PHOTOMETRIC DATA ANALYSIS

4.1 Colour–magnitude diagrams

Fig. 3 shows the $(V, U-B)$, $(V, B-V)$ and $(V, V-I)$ CMDs for all the observed stars in the cluster field. The lack of stars with $U-B$ colours with respect to those with $B-V$ and $V-I$ is really notable, which evidences the little usefulness of the ultraviolet information obtained. Our decision of acquiring U images was based on the suspicion that the cluster could be relatively young, since its field contains several bright stars projected on to a relatively fainter star field. On the other hand, it is difficult to identify accurately the cluster main sequence (MS) from the $(V, B-V)$ and $(V, V-I)$ CMDs: a crowded MS arises from the magnitude limit up to $V \sim 16$. From here to brighter magnitudes, the broad MS splits into different evolved MSs, some of which could be connected with subgiant star branches. A couple of clumps of red stars are also identified at $(V, V-I) \sim (12.5, 1.2)$, (13.2, 1.5) and their counterparts in the $(V, B-V)$ CMD. From the various evolved MSs possible, that of the cluster appears to be the one which reaches the brightest magnitudes and bluest colours. Thus, if we want to estimate the cluster fundamental parameters from its CMDs, we first should be able to disentangle the cluster MS stars from those belonging to the surrounding field. Note that both cluster and field stars are affected by nearly the same interstellar reddening, which precisely causes the overlapping of their MSs. This becomes an additional difficulty when cleaning the cluster CMDs.

4.2 Determination of the cluster centre

We started by determining the location of the cluster centre with the aim of constructing the stellar density profile, which would help to adopt the optimum cluster radius. This straightforward approach will allow us to obtain CMDs dominated by cluster stars, although some field star contamination is unavoidable. The coordinates of the cluster centre and their estimated uncertainties were determined by fitting a Gaussian distribution to the star counts in the x and y directions. The fits of the Gaussians were performed using the NGAUSSFIT routine in the STSDAS/IRAF package. We adopted a single Gaussian and fixed the constant to the corresponding background levels (i.e. stellar field densities assumed to be uniform) and the linear terms to zero. The centre of the Gaussian, its amplitude and its full width at half-maximum (FWHM) acted as variables. The number of stars projected along the x and y directions were counted within intervals of 100 pixel wide. In addition, we checked that using spatial bins from 50 to 100 pixels or from 100 to 150 pixels does not result in significant changes in the derived centre. We iterated the fitting procedure once on average, after eliminating a couple of discrepant points. The centre of the Gaussian was finally fixed at $(x_c,\ y_c)$ = (1300, 1190) pixels with a standard deviation of ±10 pixels (∼4 arcsec), equivalent to $\alpha_{2000} = 8^{\rm h}23^{\rm m}.45$, $\delta_{2000} = -29^\circ 30'.57$. We would like to mention that although there are some other concentrations of stars spread over the observed field, the one adjusted here appears to be the most notable when Gaussian amplitudes and FWHMs are considered.

Table 3. CCD *UBVI* data of stars in the field of NGC 2587. This is a sample of the full table, which is available in the online version of the article (see Supporting Information).

ID	x (pix)	y (pix)	V (mag)	$\sigma(V)$ (mag)	n_V	$U-B$ (mag)	$\sigma(U-B)$ (mag)	n_{UB}	$B-V$ (mag)	$\sigma(B-V)$ (mag)	n_{BV}	$V-I$ (mag)	$\sigma(V-I)$ (mag)	n_{VI}
...	...	...	...	...	...	...	...	...	...	...	...	...	...	...
322	202.34	177.82	19.646	0.031	1	−3.165	0.065	1	2.243	0.068	1	1.267	0.056	1
323	1286.48	178.22	18.266	0.028	3	99.999	9.999	0	1.912	0.024	2	1.073	0.038	3
324	781.27	178.33	17.551	0.034	3	1.378	0.212	2	1.571	0.051	3	0.827	0.026	3
...	...	...	...	...	...	...	...	...	...	...	...	...	...	...
...	...	...	...	...	...	...	...	...	...	...	...	...	...	...
...	...	...	...	...	...	...	...	...	...	...	...	...	...	...

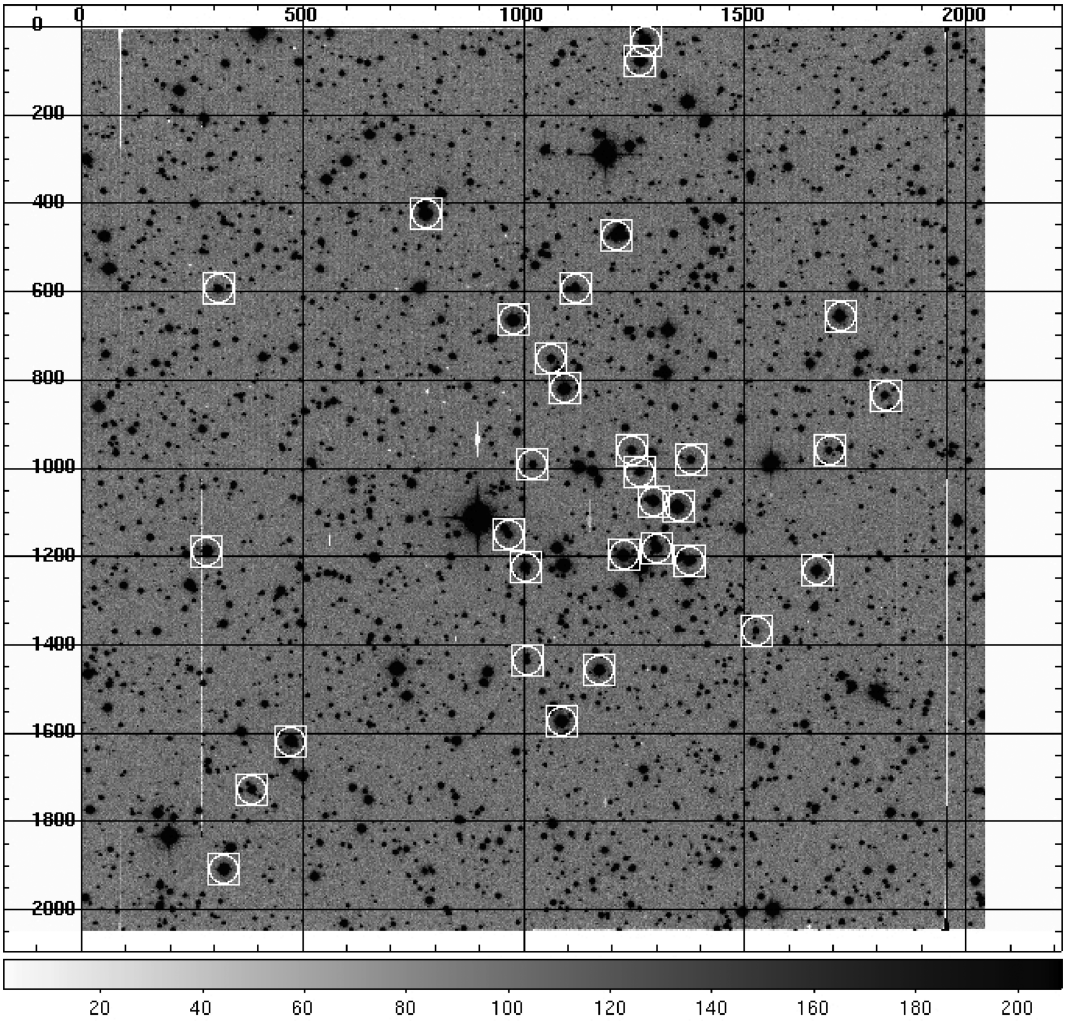

Figure 2. 200-s exposure V image of the NGC 2587 field. North is up and east is to the left. Coordinates are given in pixels. Probable cluster members are marked with an open box (see details in Section 3). The bright star close to the cluster centre is HD 70927.

This centre agrees well with that estimated by eye when the CCD images were inspected looking for the most compact main concentrations of stars. However, Palma et al. (2008) centred the cluster 1.2 arcmin to the north-east and BF07 5.9 arcmin to the south-east from our value. The centre adopted by Palma et al. (2008) was estimated by eye at the telescope when they obtained an integrated spectrum by scanning the slit across the cluster in the north–south direction to get a proper sampling of cluster stars. They assumed that NGC 2587 is a small angular size object. BF07, on his part, fitted the stellar density profile of the stars ($V \leq 15.0$) digitally identified on a $2^\circ \times 2^\circ$ *Carte du Ciel's* (1917) plate. The value he adopted corresponds to a local maximum that arises over a background level which has variations of approximately 30–40 per cent and which presents other local maxima.

4.3 Cluster morphology

NGC 2587 does not appear to be a concentrated or a rich stellar aggregate. On the contraty, bearing in mind Fig. 2 and the results obtained by BF07 and Palma et al. (2008), the apparently few cluster

Table 4. Magnitude and colour photometric errors as a function of V.

ΔV (mag)	$\sigma(V)$ (mag)	$\sigma(U-B)$ (mag)	$\sigma(B-V)$ (mag)	$\sigma(V-I)$ (mag)
11-12	<0.01	0.01	< 0.01	< 0.01
12-13	<0.01	0.02	0.01	0.01
13-14	<0.01	0.02	0.01	0.01
14-15	0.01	0.03	0.01	0.02
15-16	0.01	0.04	0.01	0.02
16-17	0.02	0.04	0.02	0.02
17-18	0.02	0.05	0.02	0.03
18-19	0.03	0.06	0.03	0.03
19-20	0.03	0.07	0.05	0.05
20-21	0.05	0.10	0.10	0.10
21-22	0.10	–	–	0.15

stars would be spread over the field, which, in turn, presents some irregularities in the stellar spatial distribution. Precisely, due to the low density and sparse distribution of cluster stars and to the populous star field on which the cluster is projected, any cluster CMD constructed from circular extractions around its centre would turn out to be highly contaminated by field stars. Fig. 4 shows that an extracted CMD from the innermost region of the cluster (upper right panel) does not allow us to distinguish easily the fiducial cluster sequence from that extracted from the surrounding cluster field (bottom right panel). Moreover, although the upper cluster MS can be delineated from a larger extracted area CMD (see e.g. bottom left panel), this one is highly contaminated by field stars.

We also cleaned statistically the $(V, B-V)$ and $(V, V-I)$ CMDs from stars that can potentially belong to the foreground/background field. In the star field CMDs, we counted the number of stars for different bins with sizes $[\Delta V,\ \Delta(B-V)] = [\Delta V,\ \Delta(V-I)] = (1.0,\ 0.2)$ mag and then subtracted the corresponding number of stars in the cluster CMDs. We divided the observed region into boxes of 250 pixels a side, and constructed for each box the corresponding $(V, B-V)$ and $(V, V-I)$ CMDs. We cleaned each box extracted CMD using, at a time, any of the remaining box extracted CMDs as a different star field CMD. Finally, we decided to adopt as a probable member of NGC 2587, any star that has at least two measures of $B-V$ and $V-I$ and, besides, which has been removed fewer than 20 per cent of the times. From the 4406 measured stars, a total of 32 fulfil such requirements. Fig. 5 shows the resulting cleaned CMDs (filled circles) superposed on to the observed ones (dots). The mere 32 probable cluster members are indicated in Fig. 2 as box encircled, while Fig. 6 shows the projected density profiles of these 32 stars in the x and y directions.

Among the observed stars brighter than $V = 12$ mag, only HD 70927 has known MK spectral type. Since this is a F7/8 II type star (Houk & Cowley 1975), its visual absolute magnitude is $M_v = -2.3$ (Straizys 1992). Assuming this star were affected by the same interstellar reddening as NGC 2587, then it would clearly be a foreground object located ∼1.4 kpc from the Sun. As for the remaining observed bright stars, their positions in the two CMDs indicate they are very unlikely to be cluster members.

We then fitted Gaussian curves to the projected density profiles in order to obtain their central positions, which turned out to be $(x_c, y_c) = (1300, 1200)$ pixels, in excellent agreement with the cluster centre as estimated in Section 4.2. Finally, we measured the angular distances from this centre to all the members. Although the radial stellar density profile of NGC 2587 does not result in a well-shaped Gaussian, the 75 per cent of the cluster members are found to be within 5 arcmin. The farthest member is located at about 8 arcmin. We adopted the latter value as a cluster radius rough estimate. Thus, the claimed compact appearance of the cluster which led Palma et al. (2008) to obtain a cluster integrated spectrum cannot be supported anymore, judging from the spatial distribution of the cluster stars. Instead, NGC 2587 seems to be a sparse OC with few quantity of members.

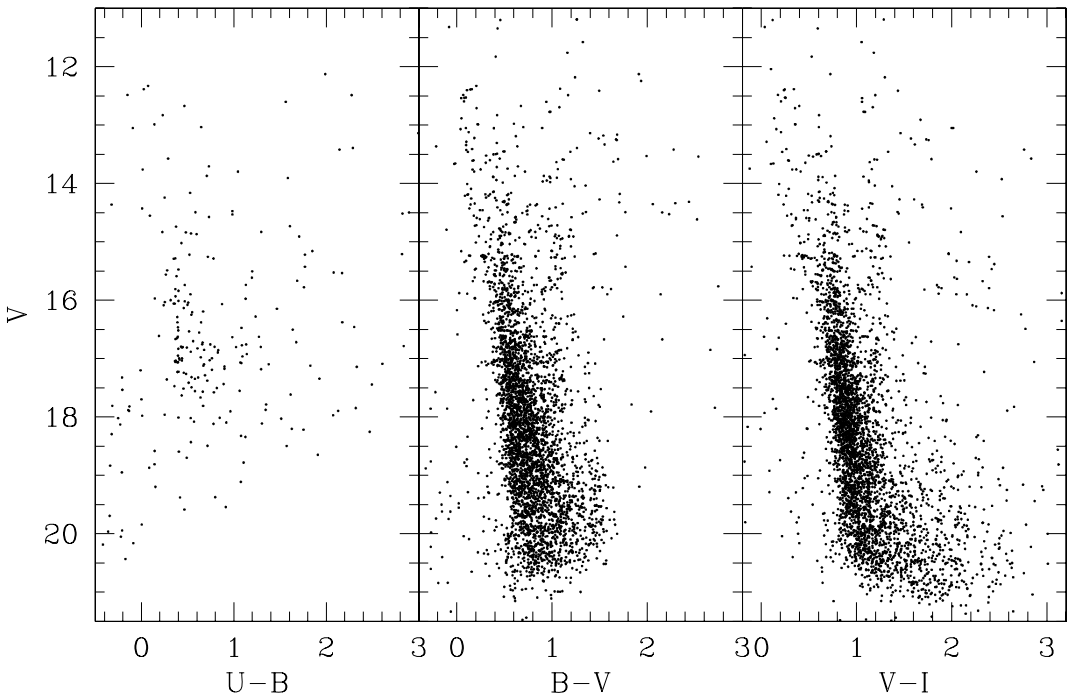

Figure 3. The $(V, U-B)$, $(V, B-V)$ and $(V, V-I)$ diagrams for the stars measured in the field of NGC 2587.

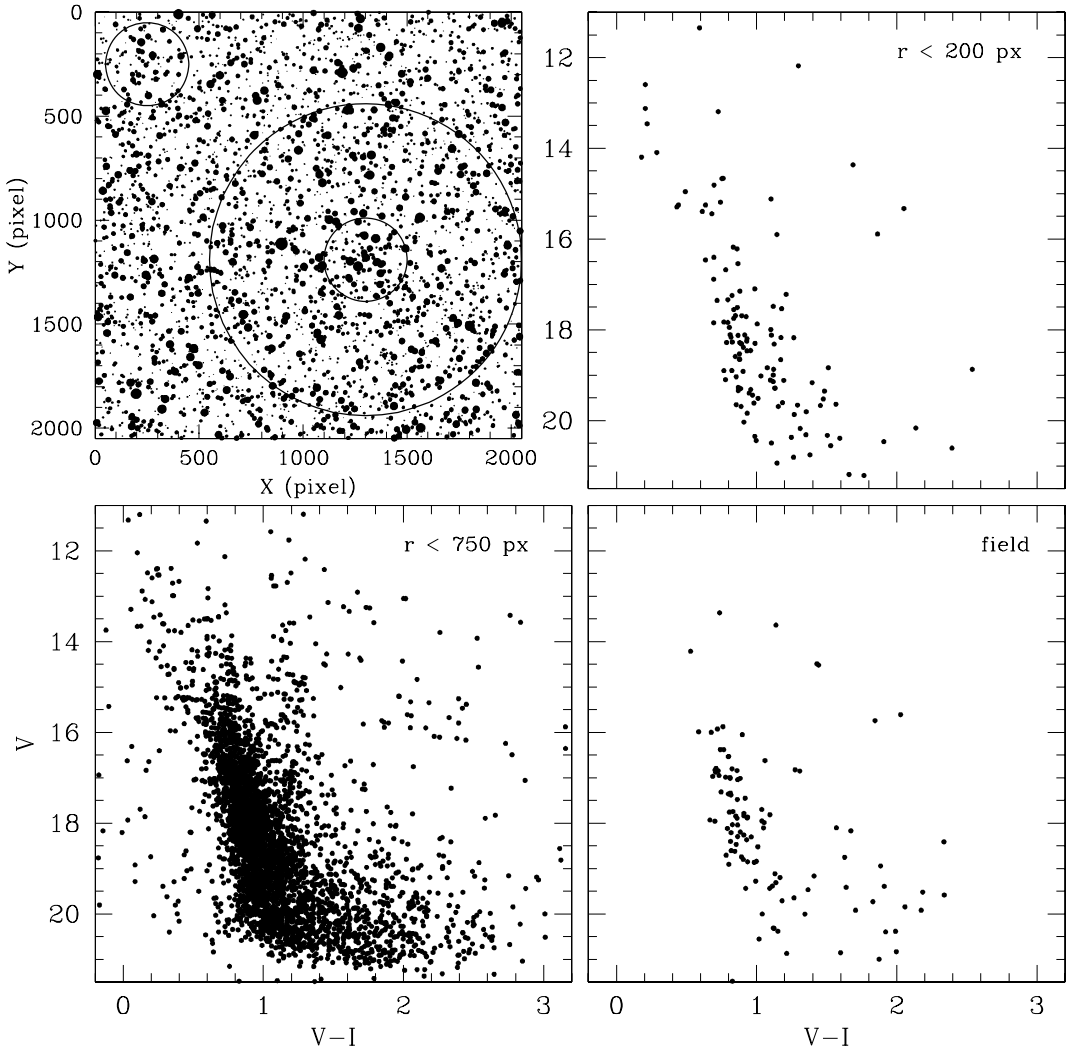

Figure 4. Schematic finding chart of the stars observed in the field of NGC 2587 (upper left panel), with two concentric circles centred on the cluster and an additional circle for the field. North is up and east is to the left. The size of the plotting symbol is proportional to the V brightness of the star. Two extracted cluster CMDs for $r < 200$ pixels (=1.3 arcmin, upper right panel) and $r < 750$ pixels (=5 arcmin, bottom left panel), and the surrounding field CMD – normalized to an area of radius $r = 200$ pixels – (bottom right panel), are also depicted.

5 CLUSTER FUNDAMENTAL PARAMETERS

The widely used procedure of fitting theoretical isochrones to the observed CMDs was employed to estimate the $E(B-V)$ and $E(V-I)$ colour excesses, the $V-M_V$ apparent distance modulus, and the age and the metallicity of NGC 2587. We fitted theoretical isochrones computed by Lejeune & Schaerer (2001) to the cleaned $(V, B-V)$ and $(V, V-I)$ CMDs. The isochrones, which cover an age range of 10^3 yr to 16–20 Gyr in steps of $\Delta \log t = 0.05$ dex, were calculated for the entire set of non-rotating Geneva stellar evolution models, covering masses from 0.4–0.8 to 120–150 $M_\odot$ and metallicities from $Z = 0.0004$ to 0.1. When selecting subsets of isochrones for different Z values to assess the metallicity effect in the cluster fundamental parameters, we preferred those including overshooting effect. Since there is no available previous estimate of the cluster metal content, we followed the general rule of starting by adopting no pre-arranged metallicity, but instead chemical compositions of $Z = 0.008$, 0.020 and 0.040 for the isochrone sets.

First, we independently fitted the zero age main sequence (ZAMS) to the $(V, B-V)$ and $(V, V-I)$ CMDs for each selected metallicity and derived the cluster colour excesses $E(B-V)$ and $E(V-I)$ and the apparent distance modulus $V-M_V$. Although the cluster MS is not very long and despite the fact that for the three Z values it is possible to find satisfactory fits, the fit for $Z = 0.020$ is the one which, as expected, best continues the non-evolved star sequence. Both metal-poorer and metal-richer ZAMSs zigzag from one side to another of the solar metal abundance ZAMS. However, the differences in colour excesses and apparent distance moduli are within 1σ error of the derived parameter errors. Still, we decided to use the isochrones corresponding to $Z = 0.020$ for the subsequent analysis.

Next, we selected isochrones of $\log t$ larger than 8.0 and used the derived pair of $[V-M_V, E(B-V)]$ and $[V-M_V, E(V-I)]$ values to estimate the cluster age. The brightest magnitude in the MS, the bluest point of the turnoff and the locus of the red giant clump were used as reference points during the fits. The isochrone of $\log t = 8.70$ ($t = 500$ Myr) turned out to be the one which most accurately reproduces the cluster features in the $(V, B-V)$ and $(V, V-I)$ CMDs. In order to match this isochrone, we used $E(B-V)$ and $E(V-I)$ colour excesses and a $V-M_V$ apparent distance

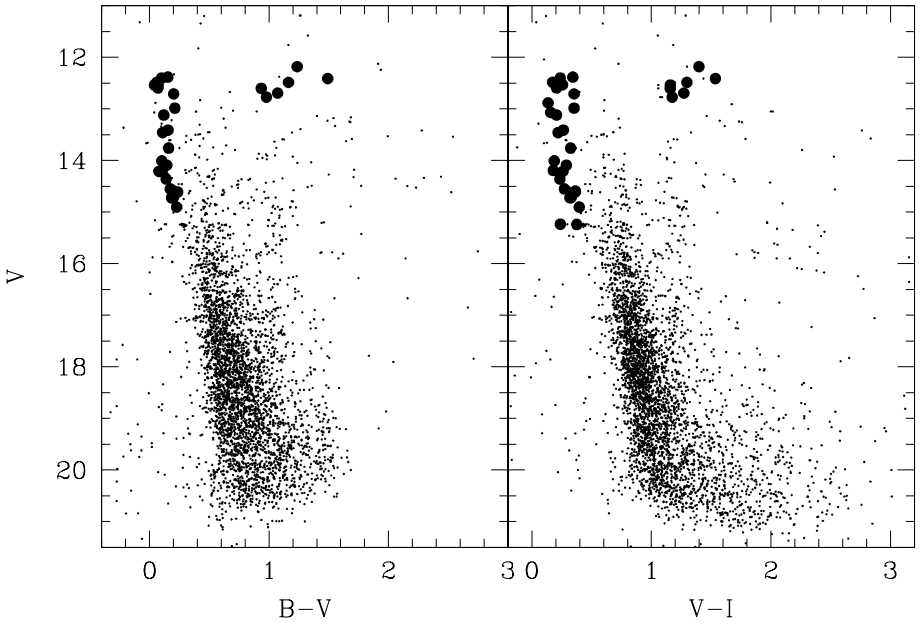

Figure 5. The $(V, B - V)$ and $(V, V - I)$ diagrams for the stars measured in the field of NGC 2587. Filled circles represent stars adopted as probable cluster members.

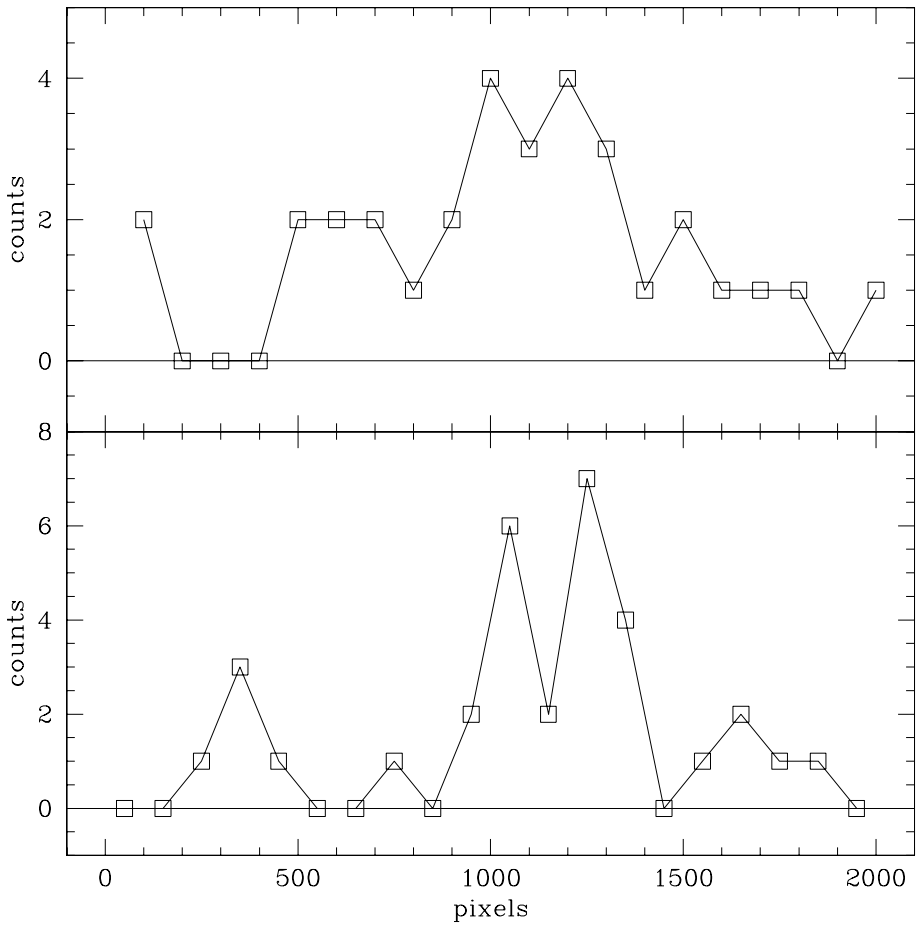

Figure 6. Stellar density profiles projected along the x (bottom) and y (top) directions for the 32 stars adopted as cluster members.

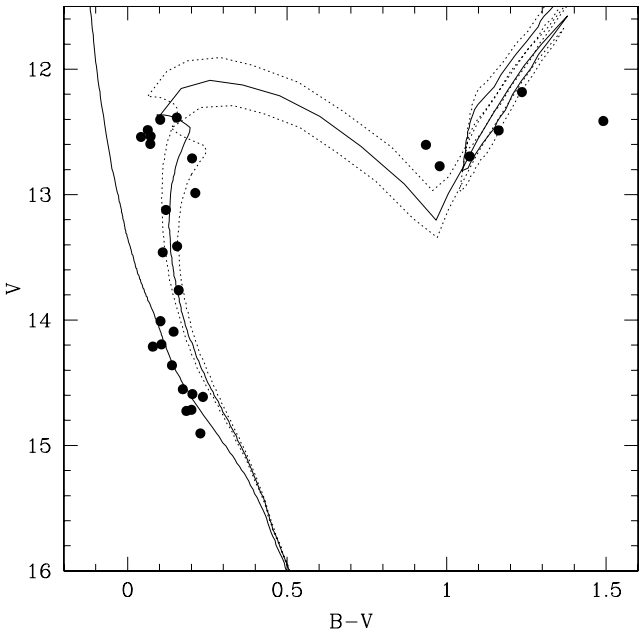

Figure 7. The (V, $B - V$) diagram for the probable member stars of NGC 2587. The ZAMS and the adopted isochrones from Lejeune & Schaerer (2001), computed taking into account overshooting, are overplotted with solid lines. For comparison purposes, we included in dotted lines the isochrones associated to the cluster age errors.

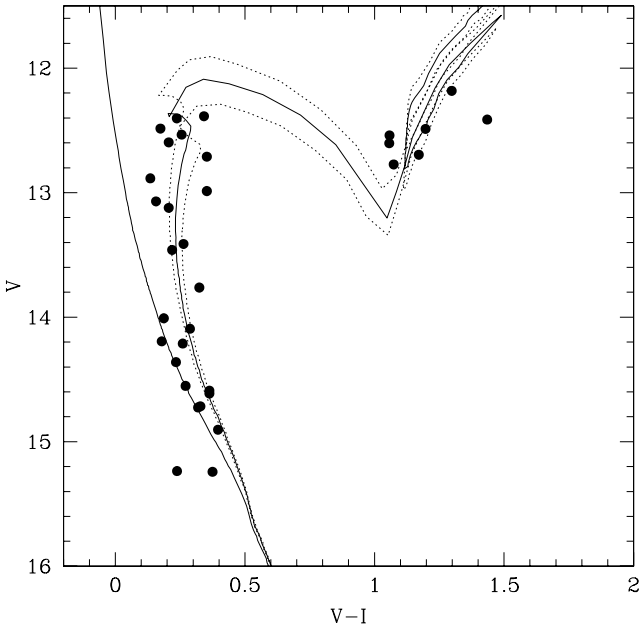

Figure 8. The (V, $V - I$) diagram for the probable member stars of NGC 2587. The ZAMS and the adopted isochrones from Lejeune & Schaerer (2001), computed taking into account overshooting, are overplotted with solid lines. For comparison purposes, we included in dotted lines the isochrones associated to the cluster age errors.

modulus of 0.10, 0.15 and 12.50, respectively, which were derived from the fit of the ZAMS. The uncertainties of these parameters were estimated from the individual values obtained from the cluster feature dispersion. Thus, we estimated $\sigma[E(B - V)] = \sigma[E(V - I)] = 0.05$ mag, $\sigma(V - M_V) = 0.25$ mag and $\sigma(t) = ^{+60}_{-50}$ Myr. In Figs 7 and 8, we overlapped the ZAMS and the isochrone of log $t = 8.70$ (solid lines) for $Z = 0.020$ to the cluster CMDs, and two additional isochrones of log $t = 8.65$ and 8.75 for comparison purposes (dotted lines).

We used the derived reddenings and apparent distance modulus and the most frequently used values for the $A_V/E(B - V)$ ratio (Straizys 1992) to obtain $V_o - M_V = 12.18 \pm 0.40$, which implies a distance from the Sun of (2.70 ± 0.70) kpc and 210 pc above the Galactic plane. The distance error was computed with the expression: $\sigma(d) = 0.46\{\sigma(V - M_V) + 3.2 \times \sigma[E(B - V)]\}d$, where $\sigma(V - M_V)$ and $\sigma[E(B - V)]$ represent the estimated errors in $V - M_V$ and $E(B - V)$, respectively. By using the cluster Galactic coordinates (l, b) and the calculated distance, we derived (9.44, −2.52, 0.21) kpc and ∼9.8 kpc for its (X, Y, Z) coordinates and Galactocentric distance, respectively, assuming the Sun's distance from the centre of the Galaxy to be 8.5 kpc.

6 ANALYSIS OF PROPER MOTIONS

BF07 measured proper motions of 4172 stars in a region of $2^\circ \times 2^\circ$ by combining stellar positions from a *Carte du Ciel's* (1917) plate with those of the USNO-B1.0 and UCAC2 catalogues. Such region contains the OC NGC 2587. We found that 20 out of our 32 probable members are in his list. Except for two stars with remarkably different μ_δ values, the remaining 18 stars have rather similar proper motions with average values of $\mu_\alpha = -4.3 \pm 3.0$ mas yr^{-1} and $\mu_\delta = -2.5 \pm 3.4$ mas yr^{-1}. This result is in excellent agreement with the membership status adopted above for these stars. For this reason, we assumed these mean values as the cluster mean proper motions. Indeed, there are only five additional stars in the BF07's list with positions within the field of view of Fig. 2, whose proper motions are similar to those of the cluster within 1σ. The bright star HD 70927, considered to be a non-member owing to its visual absolute magnitude, has a motion ($\mu_\alpha = -0.4$ mas yr^{-1}, $\mu_\delta = -2.5$ mas yr^{-1}) which differs by a little more than 1σ from the motion accepted for the cluster members.

BF07 estimated the central position of the cluster by fitting the stellar density profiles of all the stars measured in a region of $2^\circ \times 2^\circ$ along the directions of the right ascension and declination. He used a grid of 3-arcmin wide, which is ∼1/2 of the cluster radius and ∼5 times the bin size we used in Section 4.2. As expected, many peaks arise in the resulting stellar spatial distribution due both to the relatively wide grid and to the comparatively large area covered. In addition, the presence of localized groups, rows or columns of stars also contributed to produce spurious peaks. Note that the range of useful bin sizes should be constrained by the mean field stellar density. What is more, it should reflect the lower limit of the mean free path between two stars. This was not taken into account by BF07 in the case of NGC 2587. The central position finally adopted by him is 5.9 arcmin to the south-east of our value.

BF07 estimated membership probabilities for the stars with measured proper motions by constructing two distribution functions: one from stars encompassed within a circle around the cluster centre and another from a circle drawn far away from the cluster. From the comparison of both proper motion distributions, he derived membership probabilities between 50 and 70 per cent for 23 stars, which he considered cluster members. Fig. 9 shows the observed (V, $B - V$) and (V, $V - I$) CMDs with these 23 stars represented by filled circles. We included the ZAMS and the isochrone of log(t) = 8.7 as in Figs 7 and 8, for comparison purposes. As can be seen, only two stars are located along the isochrone which best reproduces the cluster features as described in Section 4.4. The remaining 21 stars apparently belong to the foreground/background field. Since

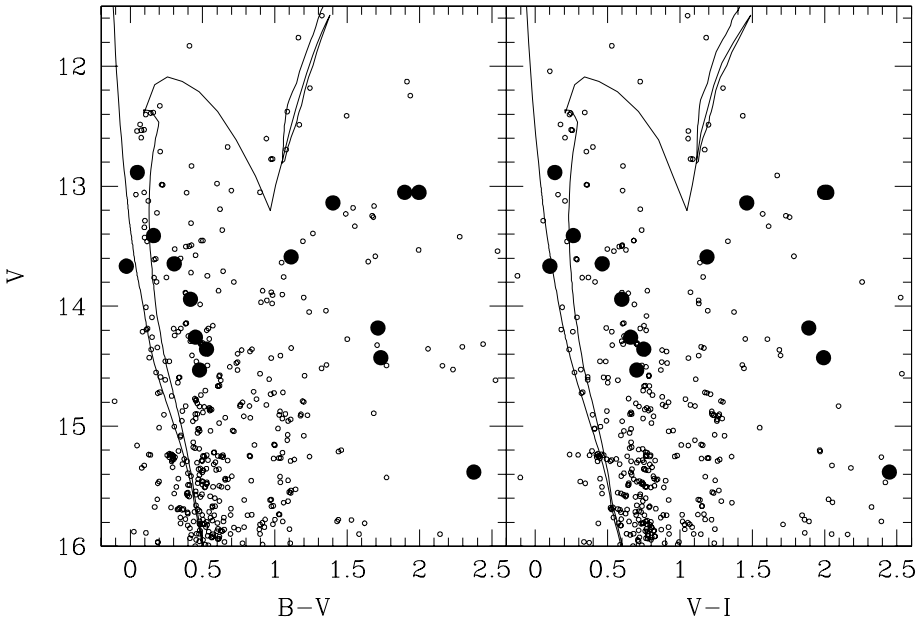

Figure 9. The (V, $B-V$) and (V, $V-I$) diagrams for stars measured in the field of NGC 2587 (open circles). Stars considered to be cluster members by BF07 are represented by filled circles. The ZAMS and the isochrone of $\log(t) = 8.7$ from Lejeune & Schaerer (2001) are overplotted with solid lines.

BF07 constructed the cluster proper motion distributions from stars spread over a region which includes part of the cluster area and part of the field region, the resulting mean proper motions do not represent those of the cluster itself, but a mixture of cluster and field proper motions. Unfortunately, BF07 did not have any photometric data available to confirm the membership probabilities he had assigned to those stars. On the other hand, their membership probabilities are far lower than the limits typically used to establish cluster membership status (i.e. $P > 80$ per cent). The results obtained by BF07 show that sometimes the sole identification of a concentration of stars in the sky is not enough to reach a conclusion about its physical nature.

7 CONCLUDING REMARKS

In this paper, we present for the first time new high quality CCD $UBVI_{KC}$ photometric data for 4406 stars in the field of the southern OC NGC 2587. These data have been used to build CMDs reaching down to $V \sim 21.0$. The analysis of the present photometric data as well as that of the available proper motions in the cluster field leads to the following main conclusions.

(i) NGC 2587 is a low stellar density object with some tens of comparatively bright members projected on to a populous star field in Puppis. We describe a new method for statistically cleaning the observed CMDs. All the observed stars brighter than $V = 12.0$, including the F7/8 type star HD 70927 ($V = 9.03$) located close to the cluster centre, are found not to be cluster members. The observed (V, $B-V$) and (V, $V-I$) CMDs, corrected by field star contamination, reveal a relatively short MS extending along $\sim$3 mag and a small group of red giant clump stars at (V, $V-I$) = (12.5, 1.2).

(ii) Estimates of the cluster fundamental parameters were performed from comparison of the observed (V, $B-V$) and (V, $V-I$) CMDs with theoretical isochrones of the Geneva group. Since the best global fits are obtained for $Z = 0.02$, we adopted this metallicity value for NGC 2587. The best-fitting isochrones yield $E(B-V) = 0.10 \pm 0.05$, $E(V-I) = 0.15 \pm 0.05$, $V - M_V = 12.50 \pm 0.25$ and an age of 500^{+60}_{-50} Myr. Therefore, NGC 2587, situated at (2.70 ± 0.70) kpc from the Sun, 210 pc above the Galactic plane and $\pm$9.8 kpc from the Galactic centre, is found to be only slightly younger than the Hyades.

(iii) The best-fitting reddening estimates support, within the errors, a normal interstellar extinction law towards the cluster direction.

(iv) From 18 probable cluster members with measured proper motions, we derived the following mean values for NGC 2587: $\mu_\alpha = -4.3 \pm 3.6$ mas yr^{-1} and $\mu_\delta = -2.5 \pm 3.4$ mas yr^{-1}.

This cluster is very interesting in the context of the chemical abundance gradient of the Galactic disc (Piatti, Clariá & Abadi 1995; Friel et al. 2002). Therefore, further study should concentrate on the confirmation of the solar metal content by means of an abundance detailed analysis of the clump stars.

ACKNOWLEDGMENTS

We thank the anonymous referee whose suggestions have helped us to improve the manuscript. This work was partially supported by the Argentinian institutions CONICET, SECYT (Universidad Nacional de Córdoba) and Agencia Nacional de Promoción Científica y Tecnológica (ANPCyT). This work is based on observations made at Cerro Tololo Inter-American Observatory, which is operated by AURA, Inc., under cooperative agreement with the NSF. We thank I. H. Bustos Fierro for permitting us to use his proper motion measurements.

REFERENCES

Alter G., Ruprecht J., Vanisek J., 1970, Catalogue of Star Clusters and Associations. Akademiai Kiado, Budapest

Archinal B. A., Hynes S. J., 2003, Star Clusters. Willman-Bell, Richmod, VA

Bonatto C., Kerber L. O., Santiago B. X., Bica E., 2006, A&A, 446, 121
Bustos Fierro I. H., 2007, Doctoral Thesis. Universidad Nacional de Córdoba, Argentina (BF07)
Chen L., Hou J. L., Wang J. J., 2003, AJ, 125, 1397
Collinder P., 1931, Medd. Lunds. Astron. Obs. 2
Friel E. D., 1995, ARA&A, 33, 381
Friel E. D., Janes K. A., Tavarez M., Scott J., Katsanis R., Lotz J., Hong L., Miller N., 2002, AJ, 124, 2693
Houk N., Cowley A. P., 1975, University of Michigan Catalogue of Two-Dimensional Spectral Types for the HD Stars. Univ. Michigan, Ann Arbor
Landolt A., 1992, AJ, 104, 340
Lauberts A., 1982, The ESO/Uppsala Survey of the ESO(B) Atlas, European Southern Observatory, Garching
Lejeune T., Schaerer D., 2001, A&A, 366, 538
Lyngå G., 1987, Catalogue of Open Cluster Data. Centre de Données Stellaires, Strasbourg
Palma T., Ahumada A. V., Clariá J. J., Bica E., 2008, Astron. Nachrichten, 329, 392
Piatti A. E., Clariá J. J., Abadi M. G., 1995, AJ, 110, 2813
Piatti A. E., Clariá J. J., Ahumada A. V., 2004a, A&A, 421, 991
Piatti A. E., Clariá J. J., Ahumada A. V., 2004b, MNRAS, 349, 641
Piatti A. E., Clariá J. J., Ahumada A. V., 2006, MNRAS, 367, 599
Stetson P. B., Davis L. E., Crabtree D. R., 1990, in ASP Conf. Ser. Vol. 8, CCDs in Astronomy. Astron. Soc. Pac., San Francisco, p. 289
Straizys V., 1992, Multicolor Stellar Photometry. Pachart Publishing House, Tucson, Arizona
Trumpler R. J., 1930, Lick Obs. Bull., 14, 154
van den Bergh S., Hagen G. L., 1975, AJ, 80, 11

SUPPORTING INFORMATION

Additional Supporting Information may be found in the online version of this article:

Table 2. Calibrated *UBVI* data of standard stars.
Table 3. CCD *UBVI* data of stars in the field of NGC 2587.

Please note: Wiley-Blackwell are not responsible for the content or functionality of any supporting meterials supplied by the authors. Any queries (other than missing material) should be directed to the corresponding author for the article.

This paper has been typeset from a TEX/LATEX file prepared by the author.